GEOPHYSICS, VOL. 54, NO. 10 (OCTOBER 1989); P. 1258–1266, 11 FIGS.

DOI:10.1190/1.1442585

Interpretation of a vertical seismic profile conducted in the Columbia Plateau basalts

J. Pujol*, B. N. Fuller‡, and S. B. Smithson‡

ABSTRACT

Seismic reflection data are often of poor quality when recorded in areas where volcanic rocks are present at or near the surface. In order to investigate this phenomenon, a vertical seismic profiling (VSP) experiment was conducted in the Columbia Plateau basalts so that the behavior of seismic energy in subsurface volcanic rocks could be observed directly, thus giving insight into data acquisition in volcanic terrains. The lithologic section at the VSP site consists of low-velocity (400 m/s to 900 m/s) alluvium in the uppermost 50 m, beneath which are layers of high-velocity (about 5800 m/s), high-density basalts interbedded with clay layers with much lower velocities (about 1700 m/s) and densities. These large velocity and density contrasts dramatically influence wave generation and propagation. In spite of the small source-borehole offset (61 m), large-amplitude *S* waves are generated by the downgoing *P* waves when they reach a shallow (250 m) clay-basalt boundary. These *S* waves, in turn, generate strong reflected *P* waves when they interact with another clay layer at 500 m. On the other hand, strong primary *P*-wave reflections are also present in the data but are affected by various interfering effects which reduce their amplitudes. The VSP data are also characterized by large-amplitude reverberations caused by seismic energy trapped in the upper 250 m of the lithologic section. Reverberations are also observed in surface data recorded near the VSP site. We conclude from our analysis that volcanic rocks, at least in the Columbia Plateau, do not exhibit unusual energy transmission characteristics and that the observations can be explained in terms of the large contrast in the elastic properties of interbedded clay and basalt.

INTRODUCTION

Seismic reflection data are often of poor quality when recorded in areas where volcanic rocks are present at or near the surface and are therefore of limited use in imaging exploration targets that lie beneath or within the volcanic sequence. Places such as the Columbia Plateau and the Rio Grande Rift in North America and the Paraná Basin in South America have hydrocarbon potential, but exploration in those places is hampered by the presence of volcanic rocks.

Little published work directly addresses the problems associated with seismic reflection profiling in volcanic terrains. Young and Lucas (1988), for example, describe a seismic experiment in the Snake River plain, Idaho, and suggest that refractions may be analyzed more easily than reflections. They also show the advantages of an interpretation combining seismic and other geophysical data, in this case magnetotelluric and gravity data.

This paper presents an interpretation of VSP data recorded in the Columbia Plateau (Figure 1), an area in the northwestern United States covered by a thick sequence of flood basalts. Reflections from depth are almost impossible to interpret on surface seismic data acquired in this region. In a shot gather (Figure 2), strong reverberating first breaks are caused in part by energy trapped in the low-velocity surface layer. These reverberations may mask any deeper reflections present in the data. The object of the VSP was to observe the propagation of seismic energy through the volcanic sequence, in order to understand better how to acquire seismic reflection data in volcanic terrains.

The data were recorded between depths of 122 m and 1082 m and were processed using a series of multichannel *f-k* filters (velocity filters) designed to reject events over a range of apparent velocities. This processing allowed separate analysis of the upgoing and downgoing wave fields and

Manuscript received by the Editor May 31, 1988; revised manuscript received April 19, 1989.
*Center for Earthquake Research and Information, Memphis State University, Memphis, TN 38152.
‡Department of Geology and Geophysics, The University of Wyoming, P.O. Box 3006, Laramie, WY 82071.

permitted us to conclude that wave propagation is not adversely affected by the presence of volcanic rocks and that numerous strong reflected waves were present in the data. However, the quality of the data is degraded by interference effects caused by large changes in velocity and density in the lithologic section. These changes in elastic parameters are also responsible for wave conversions, which were unexpected, given the small source-borehole offset (61 m). As a result of the conversions, large-amplitude P-to-S converted waves are generated, which in turn reflect as P waves.

FIG. 1. Location of the borehole where the VSP was conducted.

GEOLOGIC SETTING AND DATA ACQUISITION

The Columbia Plateau covers an area of 260 000 km^2 (King, 1977) and is characterized by a sequence of flood basalts with an average thickness of 1 km (Hooper, 1982). The basalts were deposited as a series of at least 120 individual flows between 6 m and 120 m thick that occurred episodically between 17 mybp and 6 mybp (Hooper, 1982). Between volcanic episodes, melting continental glaciers to the north of the Columbia Plateau resulted in huge floods of water sweeping across the basalts, leaving incised drainages on its surface. Later, water and eolian processes deposited sand, gravel, and loess directly on top of the basalts (Bretz et al., 1956). Also present between basalt layers are clay zones up to 30 m thick. Basalts and relatively thin sedimentary interbeds alternate to a depth of at least 2 km, as recorded during drilling of the borehole used for this VSP. This alternation juxtaposes high-velocity and low-velocity rocks, namely, basalt with a P-wave velocity of about 5800 m/s and clay and alluvial deposits with velocities as low as 1700 m/s. Densities may also be very different, about 2.9 g/cm^3 for basalt and about 2.0 g/cm^3 for clay. Relatively unlithified,

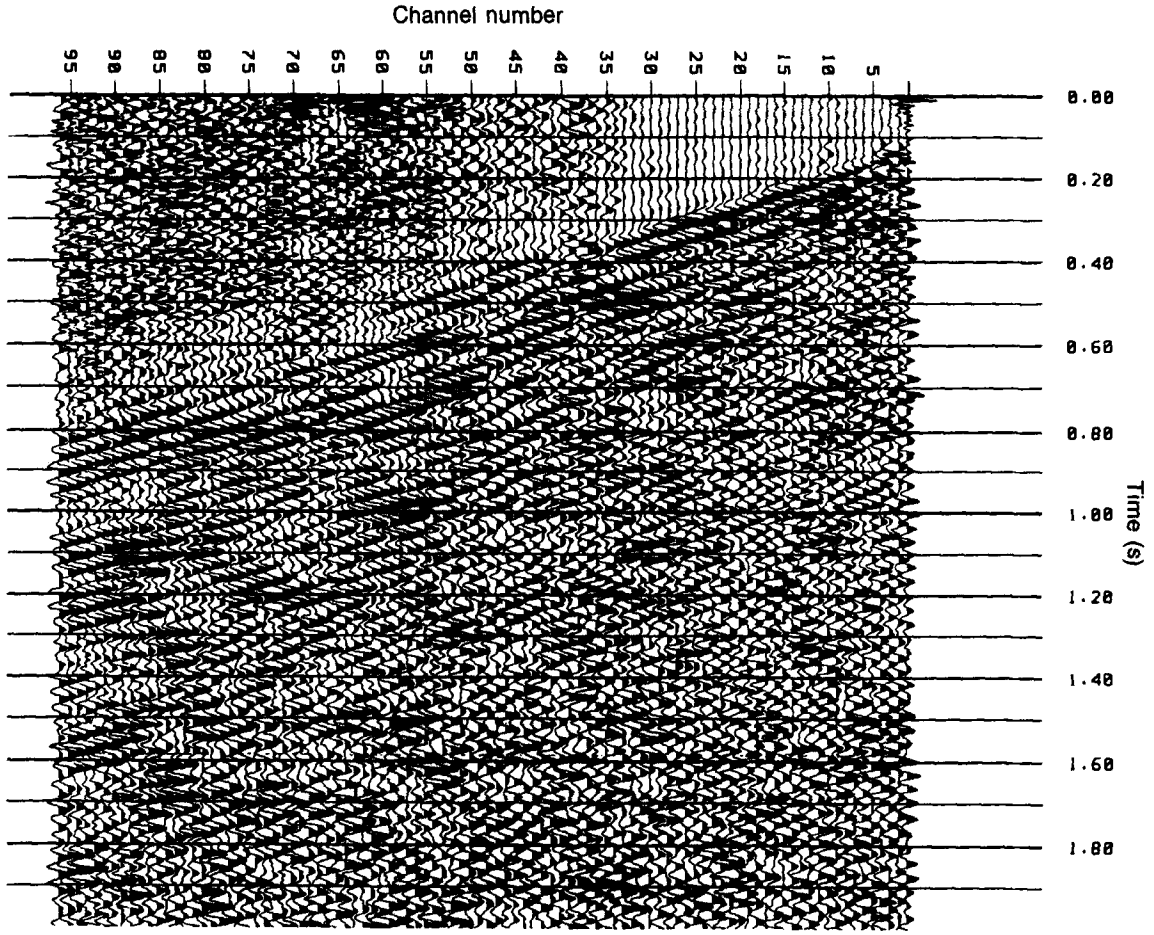

FIG. 2. A surface-seismic shot gather from the area were the VSP was recorded. A vibrator source was used. Amplitudes have been balanced using AGC with a 500 ms time gate. Note the large-amplitude reverberatory character of the first arrivals.

low-velocity (400–1000 m/s) alluvial material covers approximately 40% of the Columbia Plateau, including the VSP site, and strongly influences seismic data acquisition.

The VSP presented in this paper was recorded near the city of Moses Lake, Washington (Figure 1) in a borehole that had been drilled to a depth of 2134 m for exploration purposes but which later bridged over at a depth of about 250 m. The hole was reopened to a depth of 1082 m in order to record the VSP. Sonic and density logs were recorded when the hole was originally drilled, but a lithologic log is not available. Reasonable lithologies can be inferred, however, from the known depositional history and the log responses (Figure 3).

The VSP source was a Mertz BSX vibrator operated in the *P*-wave mode and offset 61 m from the borehole. The vibrator sweep was a nonlinear, 15 s upsweep beginning at 10 Hz and ending at 60 Hz. The downhole receiver was a Geosource/SIE SW3 three-component geophone. Nine sweeps were recorded at each depth level between 1082 m and 122 m at intervals of 15.2 m. Recording time was 18.0 s, which resulted in a crosscorrelated record length of 3.0 s. Only the upper 122 m of the borehole was cased. During the recording, several blockages occurred in the clay zones (particularly at about 250 m and 509 m), so that the hole had to be reopened three times. This information is relevant because some of our observations relate to the presence of these clay layers.

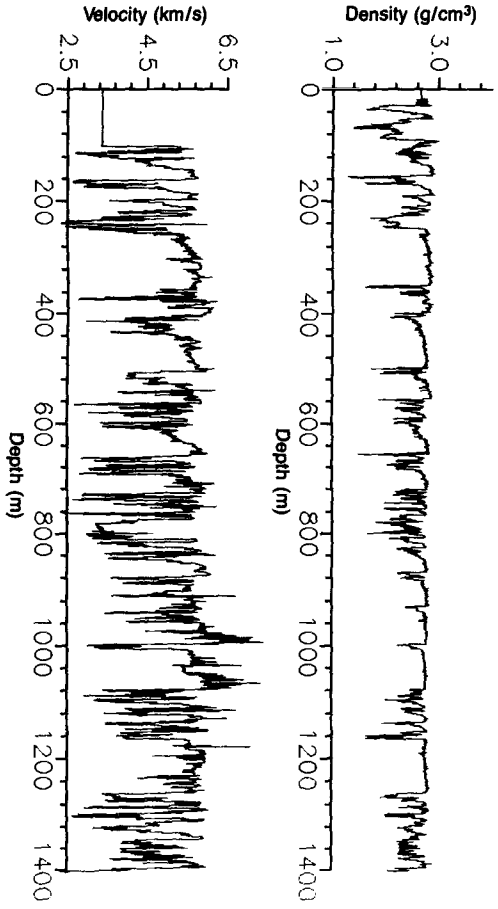

FIG. 3. Velocity and density logs for the well in which the VSP was conducted. Only the top 1400 m data are displayed. The velocity log was computed from the sonic log.

DATA PROCESSING AND INTERPRETATION

Various parts of the wave field were separated by using *f-k* velocity filters (Embree et al., 1963). These filters can be applied in two modes: pass and reject. The output of a velocity filter can be affected by the width of the pass or rejection bands in the *f-k* domain. Very narrow band-pass filters cause excessive spatial mixing of the data, so they are not recommended if one is interested in subtle waveform changes from trace to trace (Hardage, 1985). Mixing is minimized by using narrow band-reject filters. An optimum velocity filter depends, therefore, on the objectives of a given study. To isolate a particular feature, a narrow band-pass filter is very convenient; but the output is mixed substantially. Furthermore, because velocity filters may not attenuate the unwanted waves completely when they have very large amplitudes, an additional filter can be applied to further remove spurious energy. On the other hand, to analyze wave conversions and reflections simultaneously, a narrow band-reject filter to attenuate the downgoing *P* waves is more suitable.

Before presenting the processing results, we note that the quality of the data recorded on the two horizontal components is not as high as that of the data recorded on the vertical component. The likely source of the problems is that the locking arm of the downhole receiver is too weak to sufficiently couple the phone to the borehole wall, thereby resulting in excessive horizontal motion of the tool. While the horizontal-component data clearly show both upgoing and downgoing *P* and *S* waves, attempts to orient the horizontal components yielded questionable results. Furthermore, since these data do not contribute information that cannot be derived from the vertical-component data, they are not presented in this paper.

In the remainder of the paper, the VSP data of each figure are initially corrected for geometric spreading, assuming an amplitude decay proportional to the source-receiver distance. Other processing steps then follow the amplitude correction. For display purposes, the data traces for depths less than 249 m are reduced in amplitude by a factor of four because these traces are characterized by high-amplitude reverberating energy trapped between the surface and the clay layer between 220 m and 250 m. That the shallow traces are of much higher amplitude than the deeper traces is significant from the standpoint of signal-to-noise ratio in the surface data. In the surface data of Figure 2, the dominant energy is in the form of linear events that propagate with the same velocity as the first breaks. These events are caused by energy trapped in the upper portion of the lithologic section. The amplitude and duration of these reverberations are such that they can easily obliterate deeper reflections.

VSP data processing was carried out in several steps, starting with an analysis of the downgoing wave field. Below 250 m, the vertical-component data (Figure 4) are characterized by first arrivals that have very consistent signatures from one recording level to the next. Furthermore, attentuation of the peak amplitude of the *P*-wave first break between 530 m and 1080 m is about 6 dB/1000 m after

correction for spherical divergence. Attenuation rates measured in sedimentary rocks generally range between 1 and 13 dB/1000 m (McDonal et al., 1958; Hauge, 1981). This result dispels speculation that basalt, at least in the Columbia Plateau, has poor transmission characteristics.

Figure 5 shows the vertical-component data after application of two velocity filters, one to reject the downgoing *P* waves and another to reject all of the upgoing waves, thus leaving the downgoing *S* waves as the predominant waves in the filtered data. Of particular importance is the event denoted by *S*, which has an apparent velocity of 2600 m/s. This *S* wave originates at a depth of about 250 m, where it intersects the line of downgoing *P*-wave first breaks. We interpret event *S* as the result of mode conversion of the downgoing *P* wave. Later downgoing *S* waves in Figure 5 can be interpreted as the result of mode conversion of the reverberating energy trapped above 250 m depth. The converted *S* waves can also be seen in the unprocessed horizontal-component data. Significantly, these *S* waves have approximately the same peak frequency as the downgoing *P* waves (about 31 Hz). In the Discussion section we show that the mode conversions are related to the clay-basalt boundary at about 250 m.

The upgoing wave field is analyzed next. After application of a velocity filter designed to reject the downgoing wave field, the vertical-component data (Figure 6) show upgoing *P*-wave events with apparent velocities that are very close to the velocity of the downgoing *P* waves (about 5340 m/s). Figure 6 demonstrates that reflections are generated within the volcanic sequence and are efficiently transmitted by the basalt. One of the reflections (R1) originates at or just below T.D. (total depth, 1082 m) and is consistent with large changes in velocity and density near that depth (Figure 3). Surprisingly, this event travels through the lithologic sequence with little change in amplitude until it reaches a depth of about 534 m, whereupon its amplitude is severely reduced.

Another salient feature of Figure 6 is the strong event denoted by R2 which originates at about 534 m. This event is not the continuation of the weaker upgoing alignment R3, which originates at about 701 m. These events are even more clearly seen when the data of Figure 6 are velocity filtered to

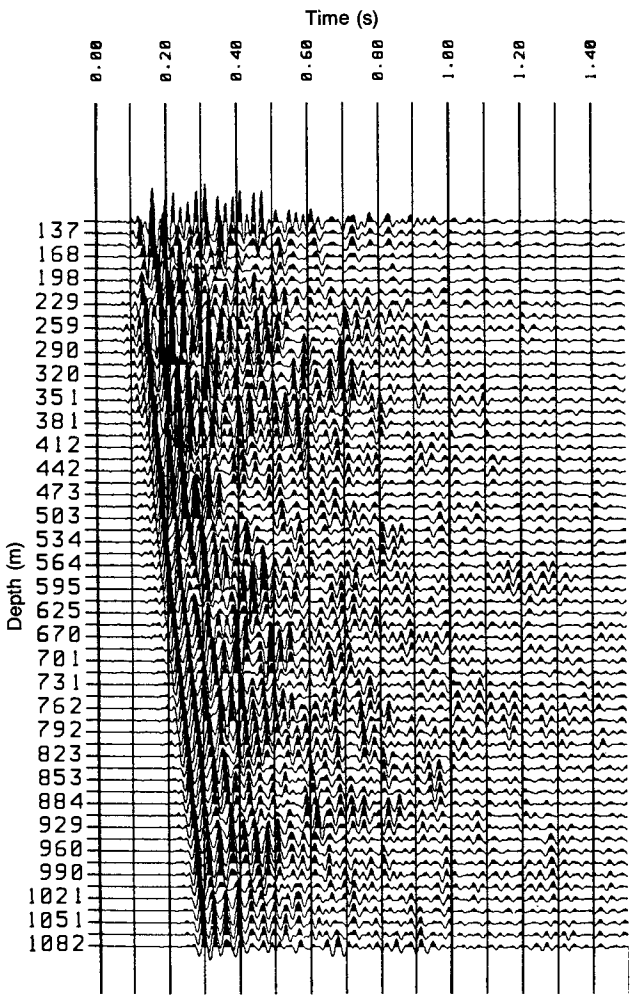

FIG. 4. Vertical-component VSP data.

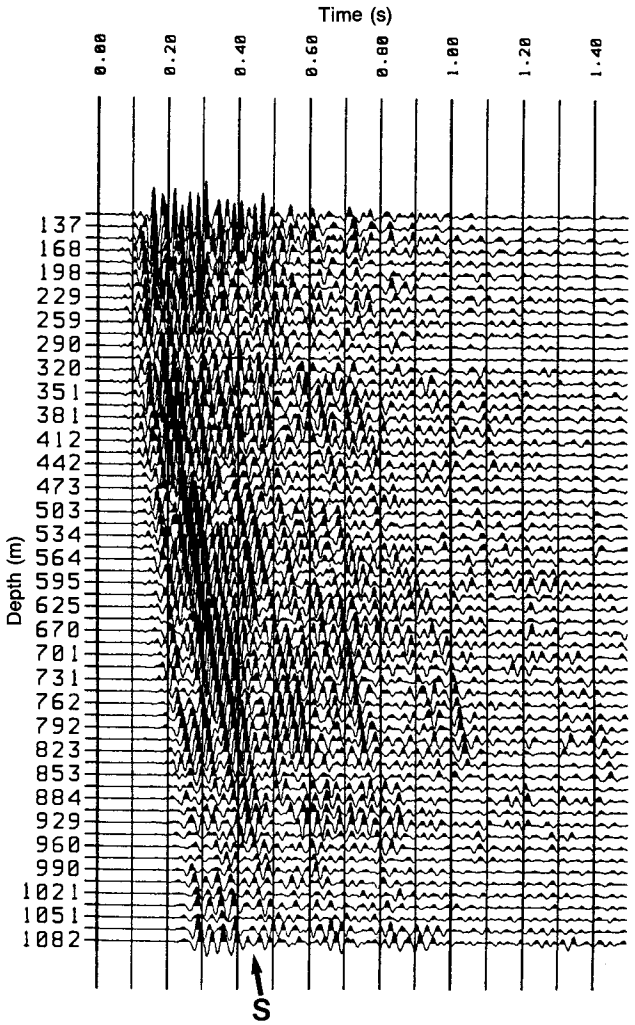

FIG. 5. Vertical-component VSP data after application of two velocity filters, one to reject the downgoing *P* waves and another to reject all the upgoing waves. Note the strong *P*-to-*S* converted wave (*S*) generated at about 250 m.

pass the *P*-wave reflections. For display purposes (Figure 7), the data thus obtained were time shifted by an amount equal to the arrival time of the downgoing *P* waves. In this way, the *P*-wave reflections align vertically. Figure 7 shows that between 701 m and 534 m, R3 consists of one or two well aligned lobes, while R2 is characterized by three or four lobes of larger amplitude. Also note that event R2 does not intersect the line of first breaks, suggesting that it is not a *P*-to-*P* reflection. This figure also shows the dramatic decrease in amplitude of reflection R1 when it reaches the 534 m level.

The origin of reflection R2 is particularly puzzling, because if it is not a primary reflection, it must be generated by reflection of a downgoing *S* wave. To explore the latter possibility, we applied to the vertical-component data a velocity filter designed to reject only the downgoing *P* waves, so that the downgoing *S* waves and the upgoing waves could be analyzed together. Event *S* in the filtered data of Figure 8 is the same *S* wave noted before (*S* in Figure 5); the arrival time of this wave at 534 m coincides with the origin time of R2. Therefore, R2 appears to be generated by reflection of the downgoing *S* waves. This interpretation is supported by a change in polarity at 534 m and between 240 ms and 300 ms. Past 300 ms, the polarity change disappears, indicating that it is not a processing artifact. The relevance of this change is discussed later. In the Discussion section we relate the origin of these reflections to the clay layer between 500 m and 525 m. This conversion is not the only one present in these data. A reflection that originates at about 381 m also appears to be caused by mode conversion (Figure 8). Here again there is a localized polarity change. The interpretation of these reflected waves as generated by an *S*-to-*P* conversion explains why these reflections do not originate at the first breaks and agrees with the observations of Lash (1980) that it is possible to have a *P*-to-*S* conversion followed by an

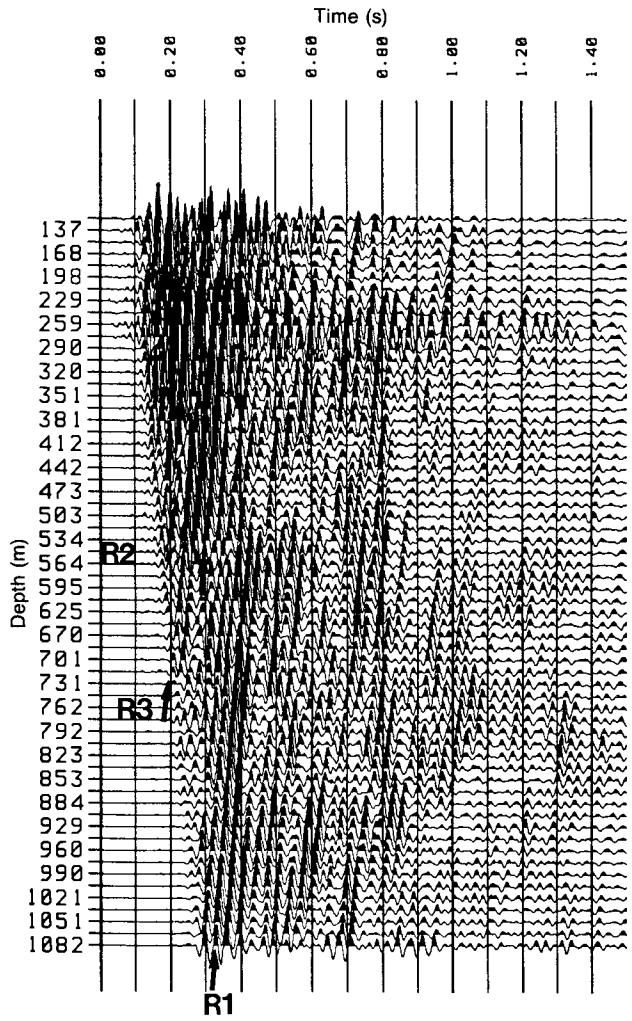

FIG. 6. Vertical-component VSP data after velocity filtering to reject the downgoing *P* and *S* waves. Note that the reflection generated just below T.D. (R1) seems to stop at about 534 m and that the strong reflection (R2) starting at this depth does not seem to be a continuation of the weaker reflection originating at about 701 m (R3).

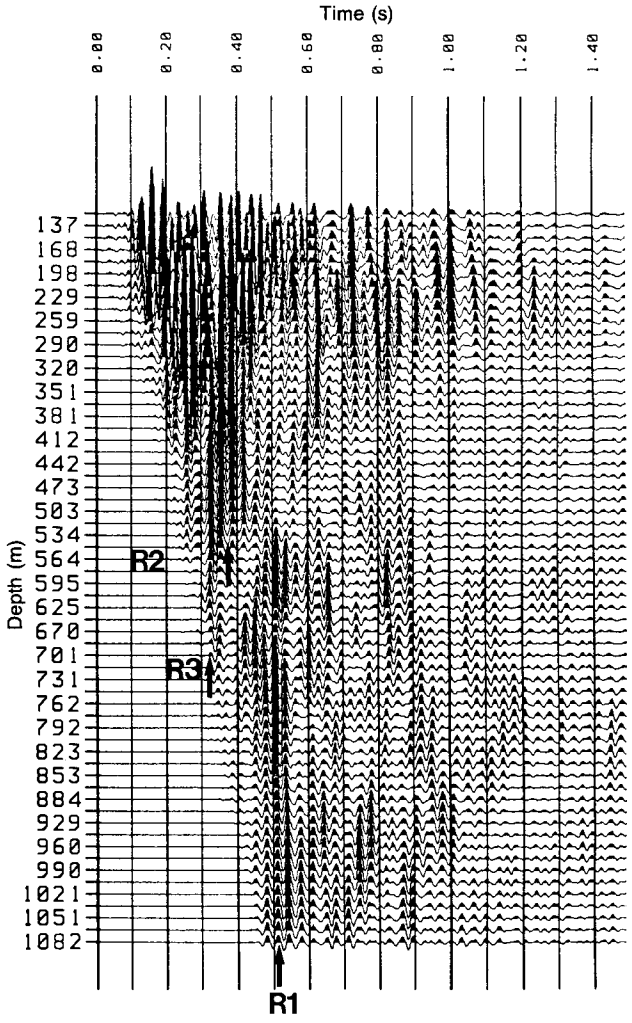

FIG. 7. Vertical-component VSP data after application of two velocity filters, one to reject the downgoing *P* waves and another to pass the upgoing *P* waves. A time shift has been applied to align the *P*-wave reflections. The observations noted in Figure 6 are seen here more clearly. Reflection R1 stops at about 534 m and reflection R2 starts at about the same depth. Reflections R2 and R3 have different character.

S-to-P conversion. Because the frequencies of the S and P waves are similar, the second conversion generates waves which resemble reflections from a P wave.

DISCUSSION

The strong mode conversions reported here are very surprising, given the small source-borehole offset (61 m) but can be explained by taking into account the large contrast in elastic properties of clay and basalt. Our analysis of the conversions is based on the use of the Zoeppritz equations (Ben-Menahem and Singh, 1981; Young and Braile, 1976), which give the amplitude of reflected and transmitted waves generated when a plane wave impinges on a plane surface of discontinuity. Note, however, that the solution of these equations gives amplitudes along the raypath. For this reason, it is necessary to multiply the amplitudes of the reflected and transmitted P wave by the cosines and the sines of the corresponding angles (as determined from Snell's law) to get the vertical and horizontal components (for S waves, multiply by the sines and cosines of the shear-wave angles instead). Use of the Zoeppritz equations requires knowledge of the P-wave velocity V_p, the S-wave velocity V_s, and the densities of the media on each side of the discontinuity. Values of V_p and density for clay and basalt were taken from the sonic and density logs. We determined values of 1700 m/s and 2.0 g/cm^3 for clay and 5800 m/s and 2.9 g/cm^3 for basalt. A V_p/V_s ratio of 2 for basalt was determined from the VSP data, but the clay layers were too thin to obtain a reliable ratio. The V_p/V_s ratio for clay is quite variable and depends on several factors, such as depth of the clay and fluid saturation. For depths of a few

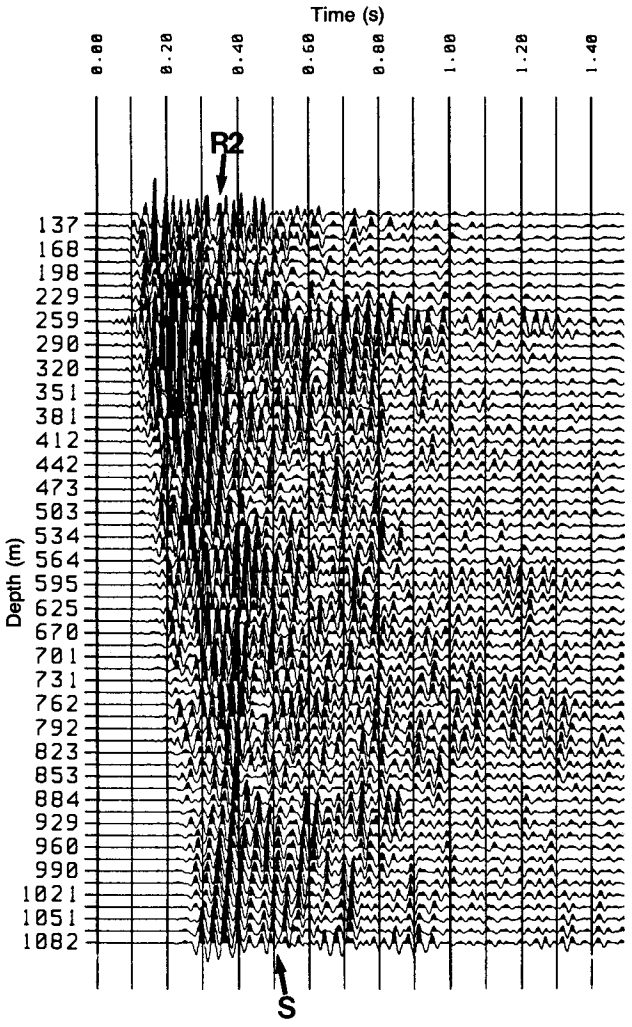

FIG. 8. Vertical-component VSP data after velocity filtering to reject only the downgoing P waves. Note the change in polarity between 503 m and 534 m in the time range 240–300 ms. The reflected P wave (R2) at that depth seems to be generated by reflection of the downgoing S wave (S).

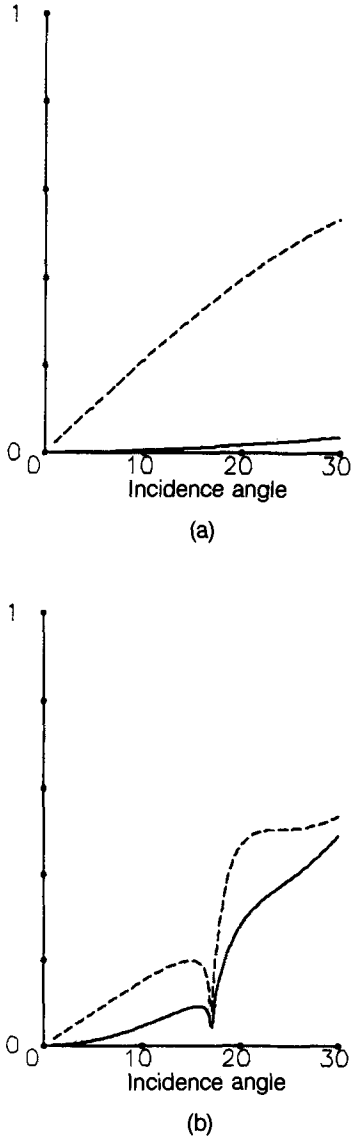

FIG. 9. Amplitudes of transmitted S waves for an incident P wave as determined from the Zoeppritz equations. The amplitude of the incident wave is 1. The solid line corresponds to the vertical component and the dashed line to the horizontal component. (a) The P-wave and S-wave velocities and densities for the incidence and transmission media are 5800 m/s, 2900 m/s, and 2.9 g/cm^3 and 1700 m/s, 680 m/s, and 2.0 g/cm^3, respectively. (b) The elastic parameters of the incidence and transmission media are as in (a) but interchanged.

hundred meters, this ratio is between 3 and 4 (Hamilton, 1976), so in the calculations that follow we used a value of 2.5. The calculations were repeated for a V_p/V_s ratio of 5; we discuss the corresponding results when they affect our conclusions.

The shallow P-to-S wave conversion is considered first. Between 220 m and 250 m there is a clay layer surrounded by basalt (Figure 3). Therefore, the mode conversion can originate, in principle, at the basalt-over-clay and clay-over-basalt interfaces. Figure 9 shows the relative amplitudes of the transmitted P and S waves as functions of the angle of incidence for the two cases. In the first case (Figure 9a), there are strong converted S waves; but they would be observed mostly in the horizontal component, which means that this interface cannot generate the observed S waves. When clay overlies basalt, there is a critical angle equal to 17° for the transmitted P wave. Above this angle, the amplitude of the transmitted S wave in the two components is substantially larger than below it. The question is whether we have incidence angles larger than the critical. To answer this question, we traced rays through a velocity model determined from surface seismic data and from VSP traveltime inversion (Pujol et al., 1986, well A) and determined that at about 250 m the angles of incidence equal or exceed 17° (Figure 10). These numbers are only approximate, since they are computed using average velocities, but nevertheless they indicate that the most likely explanation for the converted S wave is that it is generated for incidence angles larger than the critical angle for the transmitted P wave. The amplitude of the transmitted P wave is zero beyond this angle, so one may wonder how it is possible to explain both the downgoing P wave and the converted downgoing S wave. The answer is that, for a given receiver location, the raypath geometries for the two waves reaching it are different, because the transmission angle for the S wave is much smaller (closer to the vertical) than for the P wave. Therefore, for a receiver located below the clay-basalt interface, the incidence angle for a P-S raypath must be much larger than for the pure P raypath, so that it may be possible to have on the same receiver a converted S wave generated beyond the critical angle and a transmitted P wave generated at angles less than the critical. In agreement with the observations, this model predicts that the amplitude of the S wave decreases as the depth of the receiver increases.

We next consider the reflected P wave generated by the downgoing converted S wave, which is related to the pres-

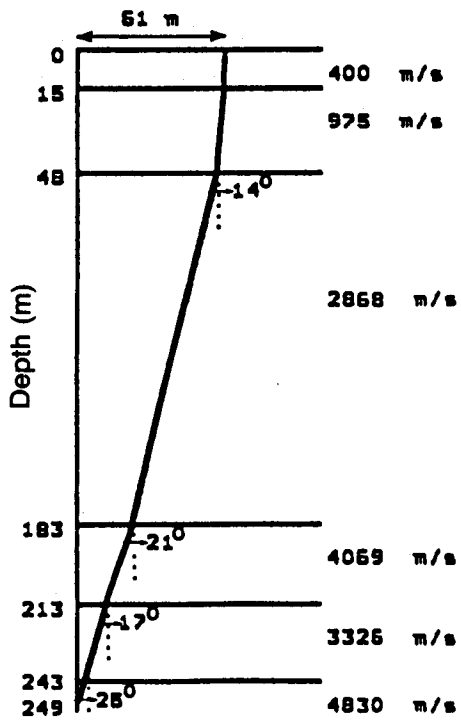

FIG. 10. Raypath for a receiver at 249 m and a velocity model determined from first arrivals (Pujol et al., 1986, Well A) and from surface seismic data.

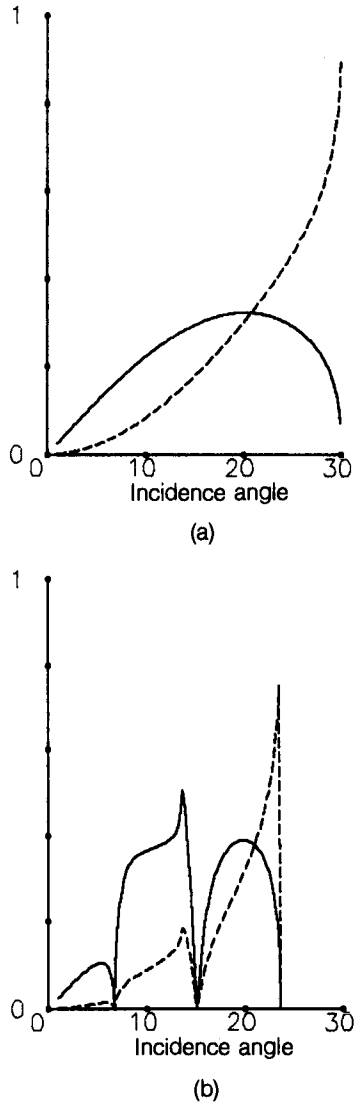

FIG. 11. Amplitudes of reflected P waves for an incident S wave as determined from the Zoeppritz equations. The amplitude of the incident wave is 1. The solid line corresponds to the vertical component and the dashed line to the horizontal component. (a) The P-wave and S-wave velocities and densities for the incidence and transmission media are 5800 m/s, 2900 m/s, and 2.9 g/cm^3 and 1700 m/s, 680 m/s, and 2.0 g/cm^3, respectively. (b) The elastic parameters of the incidence and transmission media are as in (a) but interchanged.

ence of a clay layer between about 500 m and 525 m that is surrounded by basalt. In this case the two possibilities, basalt over clay and clay over basalt, give rise to strong reflected P waves (Figure 11), but, as before, it is necessary to determine whether the incidence angles are large enough. It may seem that at about 500 m and for an offset of 61 m, these angles should be very small, but this is not the case, because now the source of S waves is at 250 m. In fact, from ray tracing through a velocity model computed from the sonic log, it is found that the incidence angle for a basalt-over-clay interface is about 14°; while for the clay-over-basalt case, the angle is close to 4°. For an angle of 14°, Figure 11a shows that the amplitude of the reflected P wave is about 0.25, which is relatively large. This number increases only slightly when a V_p/V_s ratio of 5 is used in the computations. On the other hand, Figure 11b shows that for an angle of 4°, the amplitude of the reflected P wave is considerably smaller. Beyond the critical angle for the transmitted P wave of 6.7°, the amplitude of the reflected P wave is much larger, between 0.3 and 0.4. This critical angle reduces to 3.4° for a V_p/V_s ratio of 5, but then the amplitude of the reflected P wave past this angle is smaller, about 0.2. Furthermore, regardless of the V_p/V_s ratio, between zero and the critical angle the reflected wave should have a phase shift of 180°. Past the critical angle the phase shift gets more complicated, but remains close to 180°. These phase shifts could explain the polarity change in reflection R2 mentioned before. In summary, the basalt-over-clay interface generates relatively strong P-wave reflections for a wide range of V_p/V_s ratios. The clay-over-basalt interface may or may not generate substantial reflections, depending on the V_p/V_s ratio. If the ratio is such that strong reflections are generated, they will have a delay of the order of 50 ms (depending on V_s) with respect to the reflections generated by the other interface, so that the two will combine to form a complex and wide reflection wavelet. It is not possible, however, to determine whether this is what happens in our case.

The abrupt termination of the reflection R1 (Figure 6) when it reaches the 534 m level is also very puzzling. This observation can be partly explained in terms of the clay layer discussed before. Assuming normal incidence and the values of velocity and density given earlier, the magnitudes of the reflection and transmission coefficients for the basalt-clay interface are −0.66 and 1.66, respectively. For the clay-basalt interface, the corresponding coefficients are 0.66 and 0.34, respectively. Therefore, a wave of unit amplitude impinging on the deeper interface has an amplitude of 0.56 when leaving the shallower one, a decrease of more than 40%. This reduction, although important, cannot account for the almost complete disappearance of the wave. Our interpretation is that interfering P-wave reflections generated by other converted S waves (Figure 5) also contribute to the decrease in the amplitude of the reflected wave.

The possibility that a fault between the borehole and the source affects reflection R1 is unlikely. As shown by Hardage (1985, p. 239–241), a fault generates discontinuous reflections, both in time and depth. This immediately rules out the possibility that reflections R1 and R2 are the same event offset by a fault, because R1 and R2 are continuous in depth. Furthermore, to be noticeable, the effect of a faulted reflector requires, among other things, a source-borehole offset rather large compared to the depth of the fault. This condition is clearly not met in our case. Finally, our data do not show any fault-generated diffraction effects.

There is another published example of a strong upgoing reflection that disappears before reaching the surface (Balch et al., 1982; see also Hardage, 1985, p. 342, for a cross-section). The tentative interpretation of Balch et al. (1982) was that block faulting near the borehole affected the ray-path geometry in such a way that shallow receiver locations could not be reached by reflected waves. Later, Balch and Lee (1984, p. 38) seemed to favor an explanation based on the presence of shallow high-amplitude multiples that could obscur the basement reflection, although without ruling out the effect of block faulting.

Another interesting aspect of this VSP is the relative scarcity of strong primary reflections in spite of many large velocity and density contrasts. For example, we would expect that with reflection coefficients of 0.66 at about 500 m, very strong primary P-wave reflections should be observed in the VSP data. They are not seen, probably due to interference. Consider, for example, the clay layer at 500 m, which is about 25 m thick. The downgoing P wave generates reflections from the top and the bottom of the layer. The downgoing wavelet is not simple, and resembles several cycles of a damped sine curve with peak frequency of about 31 Hz, as can be seen from the deeper traces of Figure 4. For a synthetic wavelet close in shape to the observed ones and taking into account transmission losses, we found that the resulting reflection would have an amplitude slightly less than half the amplitude of the reflection that would be generated by a single basalt-clay interface. It is important to note that if we had used a Ricker wavelet with the same peak frequency, amplitudes would not have been affected very much. In this case the two reflections would have been separated in time by such an amount that they would interfere little with each other. If we had applied Rayleigh's equation (Rayleigh, 1945; Koefoed and de Voogd, 1980), which gives the response of the layer to a vertically incident sine wave, the reduction in amplitude would have been much more severe, approximately 80%. This equation includes transmission losses and internal multiples, which are very important when reflection coefficients are large.

Additional interference effects should be expected from the alternation of high-velocity basalts and lower velocity clays and alluvial deposits. In fact, work done on wave propagation in coal seams has shown that an alternating sequence of thin low-velocity seams and higher velocity host rocks produces a very strong interfering effect, to the extent that few of the observed reflections are primaries (Van Riel, 1965; Rüter and Schepers, 1978).

CONCLUSIONS

The Columbia Plateau basalts transmit seismic energy in a manner similar to that of sedimentary rocks. The "volcanics problem" in this case is, therefore, not due to intrinsic properties of the volcanic rocks themselves. Instead, it is caused by abrupt vertical discontinuities in the elastic parameters, which affect wave generation and propagation substantially. The result is a series of effects detrimental to

the quality of seismic reflection data. These effects can be summarized as follows:

(1) Near-surface reverberations are so strong and last so long that they mask relatively strong deeper reflections.

(2) Even if deep interfaces have large reflection coefficients, the corresponding reflections may lose substantial energy at shallower strong reflectors. Destructive interference of a series of high- and low-velocity layers also contributes to the reduction of the amplitudes of reflected waves.

(3) The assumptions of normal incidence and acoustic behavior are not always warranted even for small offsets. When offsets are large, as in reflection seismology, the effect of wave conversions is even more important, and the possibility of confusing *S*-to-*P* converted waves with multiples of primary *P*-wave reflections increases. Similar conclusions were reached by Lash (1982).

(4) Some of the more prominent reflections are generated by mode conversion, and standard CDP processing may obliterate them rather than enhance them. In cases like this, it is necessary to process the data with techniques that address the geometry of the reflection raypath (Tessmer and Behle, 1988).

ACKNOWLEDGMENTS

This work was supported by the University of Wyoming Volcanic Reflection Research Project consisting of 15 oil companies. (J. Pujol also acknowledges support from the State of Tennessee Centers of Excellence program.) The VSP and CDP data were recorded by the University of Wyoming seismic crew under the direction of Chris Humphreys. The program to perform velocity filtering was written by R. Kubichek. We are pleased to thank Mertz Inc. for the loan of the BSX vibrator. The critical comments of the reviewers and the Editor helped improve the presentation of this paper.

REFERENCES

Balch, A. H., Lee, M. W., Miller, J. J., and Ryder, R. T., 1982, The use of vertical seismic profiles in seismic investigations of the earth: Geophysics, **47**, 906–918.

Balch, A. H., and Lee, M. W., Eds., 1984, Vertical seismic profiling: technique, applications, and case histories: Internat. Human Res. Dev. Corp.

Ben Menahem, A., and Singh, S., 1981, Seismic waves and sources: Springer-Verlag New York, Inc.

Bretz, J., Smith, H., and Neff, G., 1956, Channeled scabland of Washington: new data and interpretations: Bull., Geol. Soc. Am., **67**, 957–1049.

Embree, P., Burg, J., and Backus, M., 1963, Wide-band velocity filtering—The pie-slice process: Geophysics, **28**, 948–974.

Hamilton, E. L., 1976, Shear-wave velocity versus depth in marine sediments: a review: Geophysics, **41**, 985–996.

Hardage, B., 1985, Vertical seismic profiling, part A: Geophysical Press.

Hauge, P. S., 1981, Measurements of attenuation from vertical seismic profiles: Geophysics, **46**, 1548–1558.

Hooper, P. R., 1982, The Columbia River basalts: Science, **215**, 1463–1468.

King, P., 1977, The evolution of North America: Princeton Univ. Press.

Koefoed, O., and de Voogd, N., 1980, The linear properties of thin layers with an application to synthetic seismograms over coal seams: Geophysics, **45**, 1254–1268.

Lash, C., 1980, Shear waves, multiple reflections, and converted waves found by a deep vertical wave test (vertical seismic profiling): Geophysics, **45**, 1373–1411.

——— 1982, Investigation of multiple reflections and wave conversions by means of a vertical wave test (vertical seismic profiling): Geophysics, **47**, 977–1000.

McDonal, F. J., Angona, F. A., Mills, R. L., Sengbush, R. L., Van Nostrand, R. G., and White, J. E., 1958, Attenuation of shear and compressional waves in Pierre Shale: Geophysics, **23**, 421–439.

Pujol, J., Burridge, R., and Smithson, S., 1986, Velocity determination from VSP data: Tests of the method: J. Geophys. Res., **91**, 701–708.

Rayleigh, J., 1945, The theory of sound: Dover Publ. Inc., **2**.

Rüter, H., and Schepers, R., 1978, Investigation of the seismic response of cyclically layered carboniferous rock by means of synthetic seismograms: Geophys. Prosp., **26**, 29–47.

Tessmer, G., and Behle, A., 1988, Common reflection data-stacking technique for converted waves: Geophys. Prosp., **36**, 671–688.

Van Riel, W., 1965, Synthetic seismograms applied to the seismic investigation of a coal basin: Geophys. Prosp., **13**, 105–121.

Young, G., and Braile, L., 1976, A computer program for the application of Zoeppritz's amplitude equations and Knott's energy equations: Bull., Seis. Soc. Am., **66**, 1881–1885.

Young, R., and Lucas, J., 1988, Exploration beneath volcanics: Snake River plain, Idaho: Geophysics, **53**, 444–452.